Microelectronics Reliability 50 (2010) 1267–1272

Contents lists available at ScienceDirect

Microelectronics Reliability

journal homepage: www.elsevier.com/locate/microrel

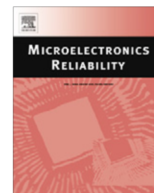

Interface traps density-of-states as a vital component for hot-carrier degradation modeling

S.E. Tyaginov [a,b,*], I.A. Starkov [c], O. Triebl [a], J. Cervenka [a], C. Jungemann [d], S. Carniello [e], J.M. Park [e], H. Enichlmair [e], M. Karner [f], Ch. Kernstock [f], E. Seebacher [e], R. Minixhofer [e], H. Ceric [c], T. Grasser [a]

[a] Institute for Microelectronics, TU Wien, Gußhausstraße 27-29, A-1040 Vienna, Austria
[b] A.F.Ioffe Physical-Technical Institute, 26 Polytechnicheskaya Str., 194021 St.-Petersburg, Russia
[c] Christian Doppler Laboratory for Reliability Issues in Microelectronics at the Institute for Microelectronics, TU Wien, Gußhausstraße 27-29, A-1040 Vienna, Austria
[d] Inst. for Microel. and Circuit Theory, Bundeswehr University, Werner-Heisenberg-Weg 39, 85577 Munich, Germany
[e] Process Development and Implementation Department, Austriamicrosystems AG, Unterpremstaetten, Austria
[f] Global TCAD Solutions, Rudolf Sallinger Platz 1, A-1030 Vienna, Austria

A R T I C L E   I N F O

Article history:
Received 2 July 2010
Accepted 13 July 2010
Available online 17 August 2010

A B S T R A C T

We refine our approach for hot-carrier degradation modeling based on a thorough evaluation of the carrier energy distribution by means of a full-band Monte–Carlo simulator. The model is extended to describe the linear current degradation over a wide range of operation conditions. For this purpose we employ two types of interface states, either created by single- or by multiple-electron processes. These traps apparently have different densities of states which is important to consider when calculating the charges stored in these traps. By calibrating the model to represent the degradation of the transfer characteristics, we extract the number of particles trapped by both types of interface traps. We find that traps created by the single- and multiple-electron mechanisms are differently distributed over energy with the latter shifted toward higher energies. This concept allows for an accurate representation of the degradation of the transistor transfer characteristics.

© 2010 Elsevier Ltd. All rights reserved.

1. Introduction

Hot-carrier (HC) degradation is associated with the build-up of defects at or near the silicon/silicon dioxide interfaced of an MOS transistor. This is due to the bombardment by carriers which have gained sufficiently high energy and are thus called “hot” carriers (see [1] and references therein). These interface states, characterized by a density N_{it}, are able to capture charge carriers and, hence, become charged. These additional charges introduced into the system are distributed along the channel and perturb the electrostatics of a transistor. Furthermore, they act as additional scattering centers thereby degrading the linear drain current I_{dlin} and the transconductance.

The current understanding of the matter is that there are two competing mechanisms responsible for silicon–hydrogen bond-breakage, i.e. the single-electron (SE) and multiple-electron (ME) processes [2,3]. As we showed in our previous work [4] even for long-channel devices with relatively high operation voltages of 5 V, the ME-process still has a substantial impact on the device degradation and both SE- and ME-mechanisms are to be considered together.

This interplay of two competing mechanisms in the context of HC degradation modeling was first proposed by the group of Hess [5,6,2,3] and then further exploited and modified by Bravaix and co-workers [7,8]. Due to the large disparity of the electron mass and the mass of the hydrogen nucleus, the only likely way to transfer a bond-breakage portion of energy by a single (hot) carrier is related to the excitation of the bonding electron to an antibonding state. This excitation then induces a force repulsing the H ion and eventually leading to its desorption.

As for the bond-breakage mechanism, presuming the interaction of bond with several carriers, the multivibrational mode excitation followed by the hydrogen release is the responsible for the bond dissociation. This mechanism was first reported for the description of the Si–H bond dissociation at hydrogenated Si surfaces. Such a dissociation has been induced by electrons tunneling from the STM tip [9–12]. Later this concept received a further application with respect to different degradation phenomena [13–15]. In fact, the driving force of these effects is the hydrogen release accompanying the Si–H bond dissociation. In the case of MOSFET reliability, these bonds are disposed at the hydrogen-annealed Si/SiO_2 interface. The mathematical formalism describing this mechanism will be presented in the next section.

* Corresponding author at: Institute for Microelectronics, TU Wien, Gußhausstraße 27-29, A-1040 Vienna, Austria. Tel.: +43 1 58801 36025; fax: +43 1 58801 36099.
E-mail address: tyaginov@iue.tuwien.ac.at (S.E. Tyaginov).

0026-2714/$ - see front matter © 2010 Elsevier Ltd. All rights reserved.
doi:10.1016/j.microrel.2010.07.030

At the same time different types of traps characterized by different density-of-states (DOS) profiles have been repeatedly reported in the literature (see e.g. [16–18]). Moreover, Hess et al. [3,19] have explained different time slopes of degradation employing different types of defects, namely SE- and ME-induced; this concept is also supported by *ab initio* calculations [20].

To summarize, rather than the total concentration of interface states generated during the HC stress, the density of charge stored in these states is important. We extend our previous approach for HC degradation modeling [4] which is based on a thorough calculation of the carrier energy distribution function (DF) by means of the full-band Monte–Carlo device simulator MONJU [21]. The model is refined in a manner to represent the evolution of the whole transfer characteristic (i.e. I_{dlin} degradation for various gate voltages V_{gs}). We demonstrate that this is possible by extraction of the DOS profiles of the two trap types. The density-of-states eventually determines the effective charge stored in the defects which determines the electrostatic and scattering contributions. Only charged traps affect the local band diagram of a transistor and play as Coulombic centers.

2. HC degradation model: basics

In this section we provide a description of our HC degradation model [4]. The model is based on the interplay of the two mechanisms of Si–H bond dissociation, i.e. of the SE- and ME-processes. We assume that these two modes may be considered independently, i.e. are described by decoupled equations and – as a result – two types of interface states are introduced.

Both SE- and ME-processes are controlled by the carrier acceleration integral which has the following functional form [3,7,8]:

$$I_{\mathrm{SE}} = \int_{E_{th}}^{\infty} f(E) g(E) \sigma_{\mathrm{SE}}(E) \nu(E) dE. \quad (1)$$

Eq. (1) is written for the SE-mechanism while for the ME-process all indexes are to be replaced by "ME". In Eq. (1), $f(E)$ is the carrier distribution function computed using the Monte–Carlo simulator MONJU, $g(E)$ the density-of-states, $\nu(E)$ the carrier velocity and σ the Keldysh-like reaction cross section, i.e. $\sigma(E) = \sigma_0(E–E_{th})^p$ with exponent $p = 11$ and $E_{th} = 1.5$ eV the threshold energy for interface state generation (σ_0 is the attempt frequency and enters the model as a fitting parameter) [3,4,7,8].

For the SE-process, I_{SE} directly enters the interface state generation rate, i.e. $\lambda_{\mathrm{SE}} = \nu_{\mathrm{SE}} I_{\mathrm{SE}}$ with ν_{SE} being the attempt rate (note that in the model instead of two parameters $\sigma_{0,\mathrm{SE}}$ and λ_{SE} we need only which is their product).

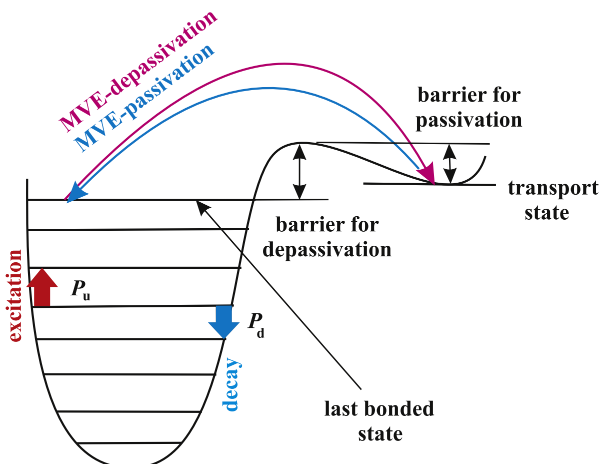

Fig. 1. The Si–H bond as a truncated oscillator. The depassivation and passivation processes are highlighted.

A Si–H bond is treated as a truncated harmonic oscillator characterized by a system of levels in the corresponding quantum well [7,8,10,15] and sketched in Fig. 1. The interface bombardment by carriers leads to the multivibrational mode excitation accompanied also by the phonon mode decay (corresponding rates are designated as P_u and P_d in Fig. 1). The bond excitation is eventually terminated when the last bonded level N_l is reached. Being settled in this level the H ion can overcome the potential barrier separating the last level N_l and the transport state thereby breaking the bond and becoming mobile. The reciprocal process when the hydrogen ion is transferred from the transport to the bonded state is linked to the bond passivation. This scenario corresponds to the ME-mechanism.

The emission from the N_l-th level to the transport state is characterized by the energetical barrier E_{emi} and corresponding Arrhenius-type rate $\lambda_{\mathrm{ME}} = \nu_{\mathrm{ME,exc}} \exp(-E_{\mathrm{emi}}/kT)$ with $\nu_{\mathrm{ME,exc}}$ being the attempt frequency (k is the Boltzmann constant and T the lattice temperature). The occupation kinetics of the levels is given by the system of equations:

$$\frac{dn_0}{dt} = P_d n_1 - P_u n_0 \quad (2a)$$

$$\frac{dn_i}{dt} = P_d(n_{i+1} - n_i) - P_u(n_i - n_{i-1}) \quad (2b)$$

$$\frac{dn_{N_l}}{dt} = P_u n_{N_l-1} - P_d n_{N_l} - \lambda_{\mathrm{ME}} n_{N_l} + P_{\mathrm{ME}} N_{\mathrm{ME}}^2 \quad (2c)$$

Here we extend the approach presented by Bravaix et al. [7,8], i.e. in the Eq. (2c) we keep the second term responsible for the bond deexcitation from level N_l to N_{l-1} level and the third term reproducing the hydrogen hopping to the transport state (the first and the fourth terms considered in [7,8] are related to the bond excitation from the N_{l-1} to N_l and to the passivation reaction, respectively). In Eq. (2) P_{ME} is the passivation rate for the ME-process and n_i is the occupation number for the i-th level. Here we assume that with overwhelming probability the bond is situated in the ground state, i.e. $n_0 \approx \sum_{i=0}^{N_l} n_i$ and thus n_0 is the total number of passivated bonds. The bond dissociation process is accompanied by the creation of the same quantity of the dangling bonds and released hydrogen atoms, i.e. $N_{\mathrm{ME}} = [\mathrm{H}^*]$ (we assume that the initial concentrations of dangling bonds and hydrogen ions are the same; otherwise the solution of Eq. (1) will be slightly modified). Note that in order to guarantee dimensionality in Eq. (2c) the rate P_{ME} is divided by n_0, i.e. $P_{\mathrm{ME}} = \nu_{\mathrm{ME,pass}} \exp(-E_{\mathrm{pass}}/kT)/n_0 = \tilde{P}_{\mathrm{ME}}/n_0$ (the prefactor for the forward rate is $\nu_{\mathrm{ME,exc}}$).

Bond excitation/deexcitation between different levels and the hydrogen transition to the transport state (and back) are characterized by enormous disparity of times and thus due to time scale hierarchy we consider these processes quasi-separately. First we treat occupation kinetics of the truncated harmonic oscillator (i.e. omitting last two terms in Eq. (2c)) and find that $n_i/n_0 = (P_u/P_d)^i$ and then we solve Eq. (2) neglecting the first two terms (the steady-state of the oscillator is already established):

$$N_{\mathrm{ME}} = n_0 \left(\frac{\lambda_{\mathrm{ME}}}{\tilde{P}_{\mathrm{ME}}} \left(\frac{P_u}{P_d} \right)^N \left(1 - e^{-\lambda_{\mathrm{ME}} t}\right) \right)^{1/2} \quad (3)$$

Note that solution (3) have the same structure (e.g. time dependence) as that demonstrated in [7] and transfers to time dependence (27) from [7] for the limit case $\lambda_{\mathrm{ME}} t \ll 1$. The probabilities of excitation/deexcitation of the Si–H bond are given by [2,7,8,22]:

$$P_u = I_{\mathrm{ME}} + w_e e^{-\frac{\hbar\omega}{kT}} \quad (4a)$$

$$P_d = I_{\mathrm{ME}} + w_e \quad (4b)$$

where I_{ME} is the carrier acceleration integral for the ME-process (it has the similar to Eq. (1) structure but characterized by parameters

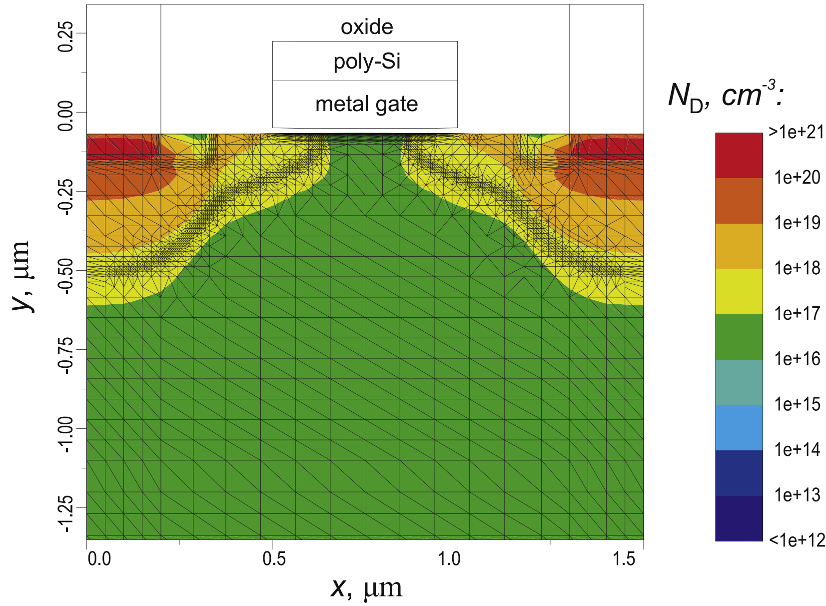

Fig. 2. The n-MOSFET architecture. The phosphorous profile is represented by the colour map.

related to the ME-process) while other parameters are phonon frequency w_e and the distance between the oscillator levels $\hbar\omega$.

As for the SE-process and corresponding bond-breakage rate λ_{SE}, the time dependence of the interface concentration related to this process is thus [22]:

$$N_{SE}(t) = n_0(1 - e^{-\lambda_{SE}t}), \quad (5)$$

where n_0 represents the total number of virgin Si–H bonds. Note that due to the stochastic nature of the bond-breakage reaction, the total concentration of interface states is thus the superposition of the SE- and ME-related contributions weighted with corresponding probabilities, i.e. $N_{it} = N_{SE}p_{SE} + N_{ME}p_{ME}$.

Only charged interface states contribute to the device performance degradation. Therefore, while modeling the transfer characteristic evolution during the HC stress one should consider effective charges stored in the interface states, not the total concentration N_{it}. These effective charges are defined as (the total charge Q_{it} is thus equal to $Q_{SE} + Q_{ME}$):

$$Q_{SE} = \int_{-\infty}^{+\infty} g_{SE}(E,x)f_{oc}(E,E_{F_n}(x)) \quad (6a)$$

$$dEQ_{MP} = \int_{-\infty}^{+\infty} g_{ME}(E,x)f_{oc}(E,E_{F_n}(x))dE \quad (6b)$$

where g_{SE} (g_{ME}) are the DOS for the SE-related (ME-) traps and f_{oc} is the carrier distribution function obtained for device operation conditions. The lateral coordinate along the interface is designated as x while E_{F_n} is the coordinate-dependent position of the quasi-Fermi level of electrons. Note that functions g_{SE}, g_{ME} are coordinate-dependent because of the normalization conditions (i.e. $\int_{-\infty}^{+\infty} g_{SE}(E,x)dE = N_{SE}(x)$, which is to be written for the ME-component just substituting indices “SE” by “ME”). Since the DOS is a position dependent function, it reflects different degradation levels in different areas of the device. The lateral coordinate also enters the DF for operation conditions because the quasi-Fermi level for carriers captured by traps is position dependent as well. The interface charge profiles generated according to the described approach are then used as input data for our device simulator MINIMOS-NT [23] to model the characteristics of a damaged device. Note that MINIMOS-NT employs simplified treatments of carrier transport with drift–diffusion and/or hydrodynamic schemes. It is worth mentioning that the drift–diffusion model maybe well suited for HV devices and for conventional MOSFETs with channel length down to ~150 nm [24] which is just the case here.

The model is thus being calibrated in order to represent the degradation of the linear drain current I_{dlin} over a wide range of stress and/or operation conditions by proper determination of $Q_{SE/ME}$. It is worth mentioning that this calibration of the model may allow us to extract the DOS associated with different types of interface states (SE- and ME-related). However, such an extraction should be supported by charge-pumping results which allow for a comparison between the simulated and experimental DOS and will be performed elsewhere.

3. Results and discussion

For the evaluation of the HC degradation model we used low voltage (LV) n-MOSFETs fabricated on a standard 0.35 µm technology depicted in Fig. 2.

The I_{ds}–V_{gs} characteristics of the virgin device are shown in Fig. 3 where the experimental curves are compared to the simulation obtained by our device simulator MINIMOS-NT [23] used within the Global TCAD Solutions framework [25]. We stressed the devices at various drain voltages V_{ds} = 6.25, 6.5, 7.0, 7.25 and

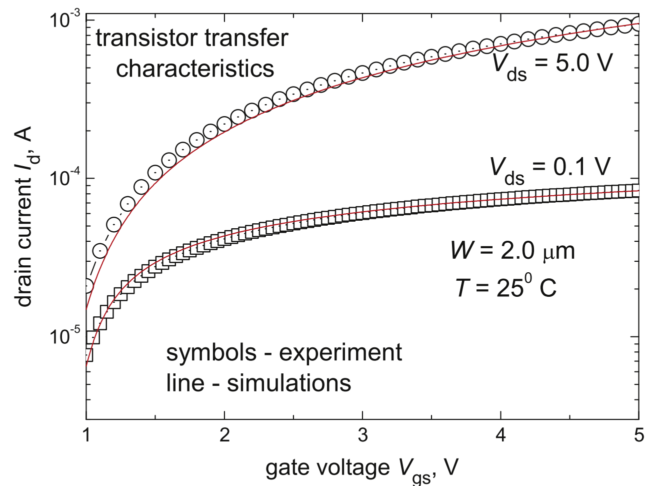

Fig. 3. The transfer characteristics of the fresh device: experiment vs. simulations.

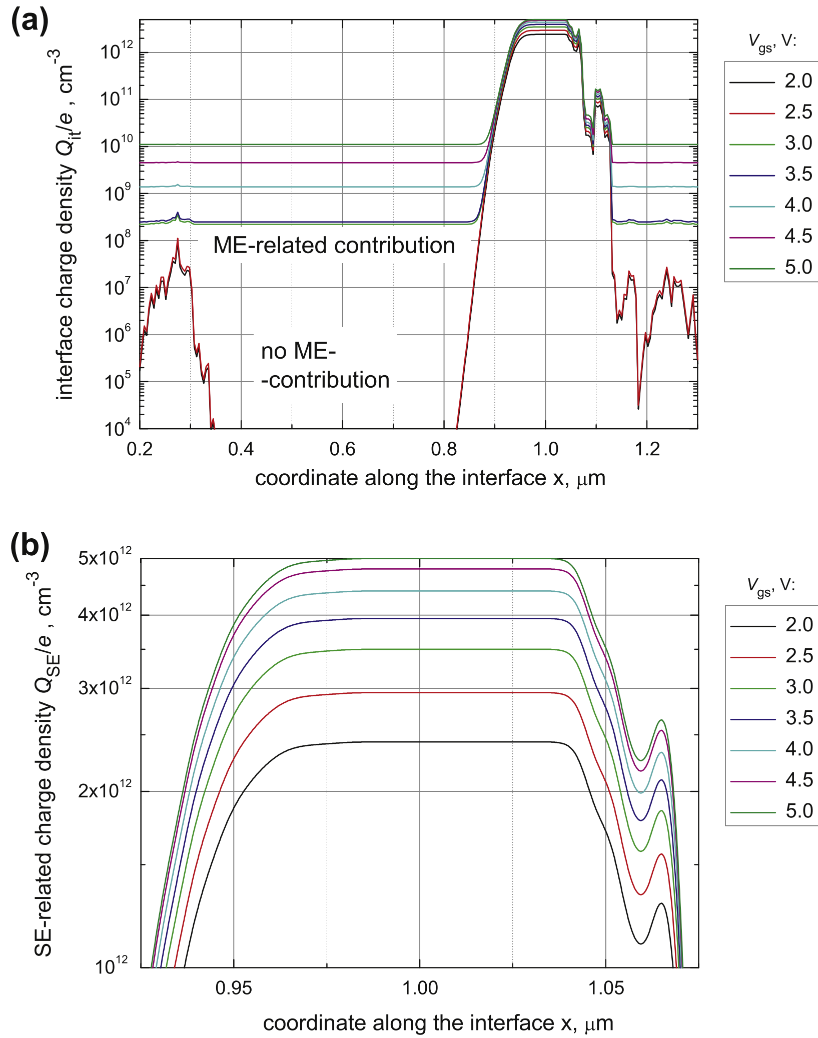

Fig. 4. The interface charge density (a) Q_{it} vs. the x-coordinate obtained for different operation conditions and (b) Q_{SE} plotted in the region of the N_{it} peak. The stress time of $t = 10$ s is taken.

7.5 V and a fixed gate voltage $V_{gs} = 2.0$ V. Devices were tested for 10^4 s at an ambient temperature of $T = 25$ °C.

An additional important component of the HC degradation is the build-up of bulk oxide charge especially in high voltage devices. In order to check whether this trapped charge does considerably contribute to the degradation of device characteristics, a set of charge-pumping measurements (not presented in this paper) has been performed. No lateral shift of the charge-pumping current (plotted against e.g. the high level of the gate pulse) with time is revealed. This circumstance supports that no build-up of bulk

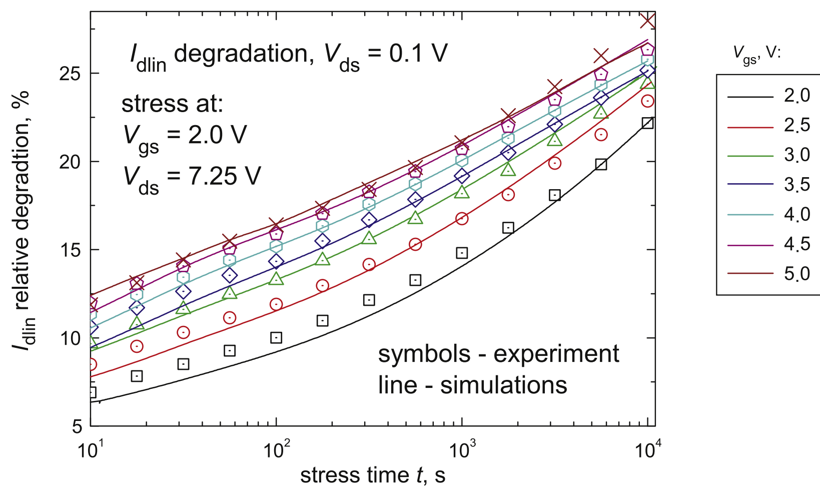

Fig. 5. I_{dlin} degradation obtained for different operating V_{gs} and for fixed stress conditions ($V_{gs} = 2.0$ V and $V_{ds} = 7.25$ V).

oxide charge occurs and the degradation is driven by generation and occupancy of the interface states.

The family of effective $Q_{it}(x)$ profiles calculated for various operation conditions (a set of gate voltages) at a fixed stress time t of 10 s is shown in Fig. 4. One can see that ME-induced defects come into play only for $V_{gs} \geqslant 3.0$. This circumstance means that the SE- and ME-related defects are differently distributed over energy and with the latter shifted to higher energies. This result agrees with the concept proposed by Hess et al. [3,19]. This approach describes the double-power law dependence of the degradation by introducing different time slopes for defects created by different processes, namely, by SE- and ME-mechanisms.

Fig. 4b resolves the density of particles captured by the SE-traps in the region where the total trap concentration N_{it} peaks vs. the lateral coordinate calculated for different V_{gs}. Since out of the N_{it} peak the main contribution to the total density Q_{it} is provided by the ME-process one may compare the behaviour of densities related to the different types of traps. For the SE-process the distance between the curves saturates, meaning that interface states of this type are almost fully occupied. In contrast, for the ME-process the increase of charge density continues indicating the fact that ME-traps are shifted to higher energies.

Fig. 4 demonstrates that the contribution of the ME-related traps pronounced even in the case of long-channel devices where the single-particle process is assumed to be the dominating one. Although the charge stored n traps is more important, the density of traps potentially can be occupied is also worth of consideration. This concentration N_{it} peaks in the region corresponding to the maximum of the acceleration integral. Due to the functional structure of the integrand Eq. (1) the maximum of this integral is shifted away respectively the electric field peak, the area where the carrier DF demonstrates most prolonged high-energy tails, etc. [4]. In the area corresponding to the maximal of I_{SE} the degradation is controlled by the SE-process, while in other device regions the ME-component plays the major role. To summarize, even in the case of long-channel devices the ME-mechanism is still present and for a proper description of the matter the superposition of these two processes is to be considered as opposed to the simplified method proposed by Bravaix and co-authors [7,8].

The model calibrated in the aforementioned manner allows us to represent the I_{dlin} degradation at various gate voltages (Fig. 5) and for different stress conditions, i.e. different V_{ds} (Fig. 6). It is worth mentioning that we do not introduce any additional fitting parameters into the model meaning that N_{it} effectively changes while switching from certain stress conditions to another. Finally, using this approach we are now able to represent the transfer characteristics of the degraded device at each time step. Fig. 7 – demonstrating measured I_{ds}–V_{gs} curves vs. the simulated ones – reveals very good agreement between experiment and theory.

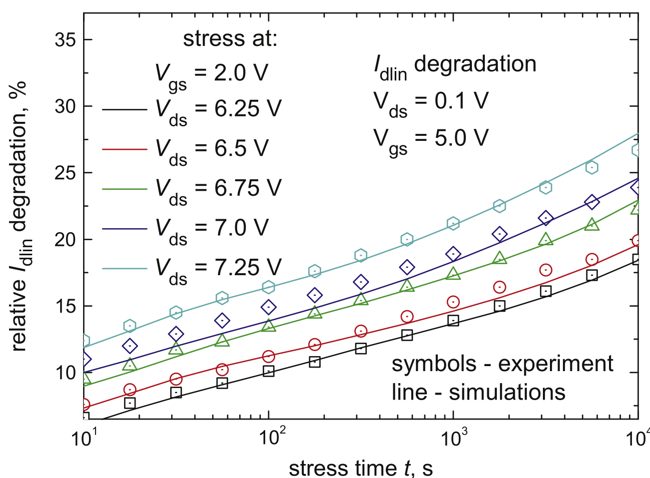

Fig. 6. Degradation of I_{dlin} obtained for different stressing V_{ds} and for fixed operating V_{gs}.

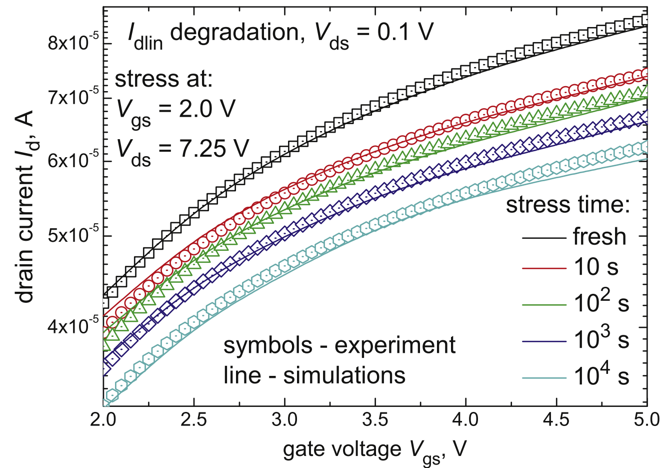

Fig. 7. The transformation of I_{ds}–V_{gs} curve during the HC stress.

4. Conclusion

Rather than the net concentration of interface states created during the HC stress for concrete device operation conditions one should consider charges trapped by these states. In fact, these charges perturb the electrostatics of transistor and act as additional scattering centers. In this work we proposed the model for HC degradation based on the assumption that the single- and multiple-carrier mechanisms of bond-breakage result in two different types of traps. These traps are characterized by different density-of-states and by different charge stored on them. The model was calibrated in order to capture the transformation of the whole I_{ds}–V_{gs} characteristic (in a wide range of stress conditions) by proper determination of these charges (Q_{SE} and Q_{ME}). Our simulations support that SE- and ME-related traps are differently distributed over energy, i.e. the latter being shifted toward higher energies. This finding agrees with the concept proposed by Hess in order to describe two different slopes of hot-carrier degradation. It is worth emphasizing that in the case of long-channel devices the ME-component cannot be neglected. In fact, the charge associated with the ME-related traps makes a profound contribution to the total degradation doze. This strategy allows us to perfectly represent the I_{dlin} degradation in a wide range of operating V_{gs}.

References

[1] Acovic A, La Rosa G, Sun YC. A review of hot carrier degradation mechanism in MOSFETs. Microelectron Reliab 1996;36:845–69.
[2] McMahon W, Haggaag A, Hess K. Reliability scaling Issues for nanoscale devices. IEEE Trans Nanotech 2003;2:33–8.
[3] Hess K, Haggag A, McMahon W, Cheng K, Lee J, Lyding J. The physics of determining chip reliability. Circ Dev Mag 2001(May):33–8.
[4] Tyaginov SE, Starkov IA, Triebl O, Cervenka J, Jungemann C, Carniello S, et al. Hot-carrier degradation modeling using full-band Monte–Carlo simulations. In: Proc 17th IEEE int symp physic failure analysis – IPFA; 2010. p. 341–5.
[5] Hess K, Register LF, Tuttle B, Lyding J, Kizilyalli IC. Impact of nanostructure research on conventional solid-state electronics: the giant isotope effect in hydrogen desorption and CMOS lifetime. Physica E 1998;3:1–7.
[6] Hess K, Tuttle B, Register F, Ferry DK. Magnitude of the threshold energy for hot electron damage in metal–oxide–semiconductor field effect transistors by hydrogen desorption. Appl Phys Lett 1999;75:3147–9.

[7] Bravaix A, Guerin C, Huard V, Roy D, Roux JM, Vincent E. Hot-carrier acceleration factors for low power management in DC-AC stressed 40 nm NMOS node at high temperature. In: Proc of Int Reliab Phys Symp – IRPS; 2009. p. 531–46.
[8] Guerin C, Huard V, Bravaix A. General framework about defect creation at the Si/SiO2 interface. J Appl Phys 2009;105:114513.
[9] Avouris Ph, Walkup RE, Rossi AR, Shen T-C, Abeln GC, Tucker JR, et al. Isotope effects and site selectivity. Chem Phys Lett 1996;257:148–56.
[10] Persson BNJ, Avourisb Ph. Local bond breaking via STM-induced excitations: the role of temperature. Surf Sci 1997;390:45–54.
[11] Stokbro K, Thirstrup C, Sakurai M, Quaade U, Hu BY-K, Perez-Murano F, et al. STM-induced hydrogen desorption via a hole resonance. Phys Rev Lett 1998;80:2618–21.
[12] Budde M, Lüpke G, Chen E, Zhang X, Tolk NH, Feldman LC, et al. Lifetimes of hydrogen and deuterium related vibrational modes in silicon. Phys Rev Lett 2001;87:1455–61.
[13] Chen Zh, Ong P, Mylin AK, Singh V, Cheltur S. Direct evidence of multiple vibrational excitation for the Si–H/D bond breaking in metal–oxide-semiconductor transistors. Appl Phys Lett 2002;81:3278–80.
[14] Ribes G, Bruyére S, Denais M, Monsieur F, Huard V, Roy D, et al. Multi-vibrational hydrogen release: physical origin of T_{bd}, Q_{bd} power-law voltage dependence of oxide breakdown in ultra-thin gate oxides. Microelectron Reliab 2005;45:1842–54.
[15] Biswas R, Li Y-P, Pan BC. Enhanced stability of deuterium in silicon. Appl Phys Lett 1998;72:3500–3.
[16] Jastrzębski C, Strzałkowski I. Reversible and irreversible interface trap centers generated at high electric fields in MOS structures. Microelectron Reliab 2000;40:755–8.
[17] Blöchl PE. First-principle calculations of defects in oxygen-deficient silica exposed by hydrogen. Phys Rev B 2000;62:6158–79.
[18] Wang Y. On the recovery of interface states in pMOSFETs subjected to NBTI and SHI stress. Solid State Electron 2008;52:264–8.
[19] Haggag A, McMahon W, Hess K, Cheng K, Lee J, Lyding J. High-performance chip reliability from short-time-tests. Statistical models for optical interconnect and HCI/TDDB/NBTI deep-submicron transistor failures. In: Proc of Int Reliab Phys Symp – IRPS; 2001. p. 271–9.
[20] Tuttle B, Van de Walle CG. Structure, energetics, and vibrational properties of Si–H bond dissociation in silicon. Phys Rev B 1999;59:12884–9.
[21] Jungemann C, Meinerzhagen B. Hierarchical device simulation. New York: Springer Verlag Wien; 2003.
[22] McMahon W, Matsuda K, Lee J, Hess K, Lyding J. The effects of a multiple carrier model of interface states generation of lifetime extraction for MOSFETs. Int Conf Mod Sim Micro 2002;1:576–9.
[23] MINIMOS-NT Device and Circuit Simulator, User's Guide, Institute for Microelectronic, TU Wien.
[24] Grasser T, Jungemann C, Kosina H, Meinerzhagen B, Selberherr S. Advanced transport models for sub-micrometer devices. In: Proc of Int Conf Simulation Semicond Proc Dev – SISPAD; 2004. p. 1–8.
[25] http://www.globalTCADsolutions.com.